Applied Surface Science 364 (2016) 896–908

Contents lists available at ScienceDirect

Applied Surface Science

journal homepage: www.elsevier.com/locate/apsusc

Protein-resistant properties of a chemical vapor deposited alkyl-functional carboxysilane coating characterized using quartz crystal microbalance

Shyam V. Vaidya [a,*], Min Yuan [b], Alfredo R. Narváez [a], David Daghfal [c], James Mattzela [b], David Smith [b]

[a] Diluent Research & Formulation, Diagnostics R&D, Abbott Laboratories, 100 Abbott Park Road, Abbott Park, IL 60064, USA
[b] SilcoTek® Corporation, 225 PennTech Drive, Bellefonte, PA 16823, USA
[c] ADD Technical Services, Abbott Laboratories, 100 Abbott Park Road Abbott Park, IL 60064, USA

ARTICLE INFO

Article history:
Received 6 April 2015
Received in revised form
30 November 2015
Accepted 12 December 2015
Available online 15 December 2015

Keywords:
Carboxysilane coating
Protein
Adsorption
Biofouling
Dursan
QCM-D

ABSTRACT

The protein-resistant properties of a chemical vapor deposited alkyl-functional carboxysilane coating (Dursan®) were compared to that of an amorphous fluoropolymer (AF1600) coating and bare 316L grade stainless steel by studying non-specific adsorption of various proteins onto these surfaces using quartz crystal microbalance with dissipation monitoring (QCM-D). A wash solution with nonionic surfactant, polyoxyethyleneglycol dodecyl ether (or Brij 35), facilitated 100% removal of the adsorbed bovine serum albumin (BSA), mouse immunoglobulin G (IgG), and normal human plasma proteins from the Dursan surface and of the adsorbed normal human plasma proteins from the AF1600 surface, whereas these proteins remained adsorbed on the bare stainless steel surface. Mechanical stress in the form of sonication demonstrated durability of the Dursan coating to mechanical wear and showed no negative impact on the coating's ability to prevent adsorption of plasma proteins. Surface delamination was observed in case of the sonicated AF1600 coating, which further led to adsorption of normal human plasma proteins.

1. Introduction

Prevention of non-specific protein adsorption to surfaces is highly important for the technological performance of many products in the food, marine, and medical industries, to name a few [1,2]. No doubt, the level of acceptable non-specific protein loading could greatly depend on the specific technology and industry requirements. For example, medical devices in the modern clinical laboratory widely utilize immunoassay formats that amplify the detection of relevant analyte found in whole blood, serum, plasma, cerebral spinal fluid, urine, and other bodily fluids. Although the use of immunoglobulins allows for highly sensitive and specific capture of the molecules of interest, the potential interference from non-specific binding (NSB) of unwanted molecules to the solid surfaces surrounding the antibodies often limits performance claims, such as limit of detection (LOD) because of a poor signal to noise ratio [3]. In addition to the negative impact that sample or reagent protein NSB may cause during the immuno-detection of analyte, much concern still exists with the prevention of key reagent protein loss to surfaces in manufacturing containers (usually made up of stainless steel), fill tubing, packaging (usually hydrophobic surfaces), and automated analytical systems (that may contain stainless steel parts). For example, automated analytical systems pipettes could non-specifically bind traces of immunoglobulins that will eventually be carried on to a different part of the system thus generating cross-reagent contamination and interference. To mitigate these problems, automated systems may incorporate special coatings that sustain continued use, exposure to a high variety of chemical formulations, and preventive maintenance procedures that involve harsh washes by solutions containing caustic chemicals.

A commonly used substance to impart protein adsorption resistance to a surface is based on oligo- or poly (ethylene glycol) (PEG), with inertness or non-fouling properties attributed to a hydrophilic nature. Although the mechanism of resistance to adsorption of proteins remains inconclusive, it is well believed that the strong interaction of the surface with water plays a key role. In fact, Whitesides' group proposed a set of design principles for inert surfaces which includes hydrophilicity, the presence of hydrogen-bond acceptors, the absence of hydrogen-bond donors, and overall electrical neutrality [4]. However, PEG is not stable and has a

* Corresponding author.
E-mail address: shyam.vaidya@abbott.com (S.V. Vaidya).

http://dx.doi.org/10.1016/j.apsusc.2015.12.086
0169-4332/

tendency to auto-oxidize in the presence of oxygen and thereby loses its protein-resistance characteristic [2,5].

Another class of coatings that are used to resist biofouling consists of hydrophobic surfaces such as PDMS (polydimethylsiloxane) and PTFE (polytetrafluoroethylene) surfaces [2,6]. These surfaces are known to show good "fouling release" properties, due to the low modulus and low surface energy that allow the easy detachment of adhered fouling species [2]. These polymer surfaces, however, often have delamination issues during use, rinsing, and physical wear. An alternative coating solution that offers better physical stability as well as chemical stability in air, liquids and other oxidative environments is highly desirable.

In this paper, we used the quartz crystal microbalance with dissipation monitoring (QCM-D) [7,8] to characterize the protein resistant anti-biofouling properties of a chemical vapor deposited alkyl-functional carboxysilane coating (Dursan® [9,10]) on a stainless steel surface via non-specific adsorption of different biological macromolecules. QCM-D monitors changes in oscillation frequency and dissipation of a planar crystal substrate upon adsorption of macromolecules [7,8]. Two very common immunoassay blocker proteins (i.e. bovine serum albumin (BSA) [11] and mouse Immunoglobulin G (mouse IgG) [12]), a synthetic amino acid polymer poly-L-lysine hydrobromide (PLL) [13], and normal human plasma (NHP) – representing patient samples (with a mix of albumins, globulins, and other serological proteins [14]), all at concentrations relevant to immunoassay reagent formulations, were utilized to determine the non-specific adsorption of protein on coatings made up of Dursan, 316L grade stainless steel (SS), and AF1600 – an amorphous fluoropolymer surface. A stainless steel coated QCM-D sensor was used as the substrate to characterize antifouling properties of the Dursan coating as prolonged adsorption of BSA on SS has been shown to cause biofouling through protein-induced enhancement of metal release from stainless steel [15,16]. Impact of a nonionic surfactant, Brij 35 that is used in generic immunoassay wash buffer formulations on protein adsorption was studied. Sonication was employed to induce rapid mechanical wear and evaluate durability of the coating adhesion to the QCM-D sensor substrate. Protein adsorption on the sonicated QCM-D sensors with coatings was further evaluated.

2. Experimental

2.1. Materials

Bovine serum albumin (BSA; SKU # 68100) and mouse immunoglobulin G (mouse IgG; SKU # A66184M-ASR) were purchased from Proliant Biologicals, Inc. (Boone, IW, USA) and Meridian Life Science, Inc. (Memphis, TN, USA), respectively. Poly-L-lysine (PLL; mol. wt. ~9000) was purchased from Sigma. Normal Human Plasma manufactured by Abbott Laboratories was used as received. A 10 mM phosphate buffer saline (PBS) solution with 0.15 M NaCl at pH 7.2, was used to prepare solutions of 1% BSA, 1% mouse IgG, and three different concentrations of PLL. pH of each protein solution was adjusted to 7.2 ± 0.1. Antimicrobial agent Sodium Azide (Charkit Chemical Corporation, CT, USA) was added into each protein solution at 0.1% (w/v) for longer shelf life at 2–8 °C. PBS with a nonionic surfactant – polyoxyethyleneglycol dodecyl ether (Brij 35) at 0.05% (w/v) and 0.1% sodium azide was used to obtain the baseline and rinse measurements in QCMD experiments. The solution has henceforth been identified as *WB1*. PBS without surfactant will be identified as *WB2*. CHROMASOLV® Plus grade water (HPLC water) was purchased from Sigma–Aldrich, Inc. (St. Louis, MS, USA) and was used for cleaning of sensors, Q-Sense assembly and preparation of different cleaning solutions. Hellmanex™ – a cuvette cleaning concentrate was purchased from Sigma–Aldrich, Inc., Deconex® 11 UNIVERSAL (SKU # NC0361563) was purchased from Fisher Scientific, Inc.

2.2. Coatings

Protein adsorption on different surfaces of interest was studied using *Q-Sense E4* – a quartz crystal microbalance with dissipation monitoring (or QCM-D) from Biolin Scientific, Inc. (Linthicum Heights, MD, USA). AT-cut quartz crystal sensors with base resonance frequency of 5 MHz and coated with a uniform thin layer of 316L grade Stainless Steel (QSX 304), and AF1600 (QSX 331) – an amorphous fluoropolymer – were purchased from Biolin Scientific, Inc.

Stainless steel (SS) sensors were further coated by a proprietary deposition called Dursan. Dursan is applied via a 3-dimensional chemical vapor deposition process involving the decomposition of an alkylsilane followed by an oxidative exposure of the base material [9,10]. The surface is then functionalized with a second alkylsilane to give a wear-resistant, hydrophobic and chemically inert coating. The spectroscopically determined coating thickness using a Filmetrics F20 instrument was about 200–300 nm on the QCMD sensors, and it exhibited a static water contact angle of 85–90° (measured with a ramé-hart model 200 standard goniometer). The water contact angle on the as-received (uncoated) SS sensor was ~72° which decreased to ~52° after the SS sensor cleaning steps described in Section 2.4. Water contact angle on the as-received AF1600 sensor was ~120°.

2.3. Surface XPS and SIMS analysis of Dursan coating

The SIMS (Secondary Ion Mass Spectroscopy) measurements were conducted at Evans Analytical Group (East Windsor, NJ) using Cesium (Cs) primary ion bombardment, and Cs attached positive secondary ions were detected. The XPS (X-ray photoelectron spectroscopy) analysis was conducted at the Pennsylvania State University's Materials Characterization Lab using a Kratos Analytical Axis Ultra spectrometer with a monochromatic Al Kα source. The scan was collected at a pass energy of 80 eV with a 1 eV step size.

2.4. QCMD characterization

Protein solutions were flowed over sensors maintained at 25 ± 0.1 °C using a peristaltic pump (Ismatec IPC-N4) assembly attached with the *Q-Sense E4* unit. (The unit allows 4 distinct measurements in parallel.) Details of the working principle and data acquisition using QCM-D can be obtained from these referenced publications [7,8]. In brief, changes in frequency (Δf) and dissipation (ΔD) at the 3rd, 5th, 7th and 9th overtones of the base resonance of Quartz crystal (5 MHz) were monitored over time.

Base resonance of each sensor was first determined in air. Each sensor was then exposed to WB1 at 0.150 mL/min flow rate for up to 2 h. This step was performed to ensure complete removal of any residual contaminants from the coatings as well as priming of the surfaces before exposure to proteins. Experiment baseline was determined by flowing WB1 over all sensors for ~4 min. Protein solution of interest was then flowed over the sensors for ~20–25 min and was followed by rinse using WB1 for another 25 min. All experiment steps were conducted at 0.150 mL/min flow rate. At the end of each experiment, per the supplier recommendations, cleaning of the modules was conducted by flowing 2% Hellmanex™ solution for ~30 min followed by HPLC water for ~2 h, both at 1 mL/min. Sensors were further cleaned using the protocols recommended by Biolin Scientific. Stainless steel (SS) sensors were cleaned after each experiment by storing in a 1% solution of Hellmanex™ in HPLC water for a minimum of 30 min followed by

thorough rinse with HPLC water, sonication for 10 min in 190 proof ethyl alcohol, drying by nitrogen gas, and exposure to UV/Ozone treatment (BioForce Nanosciences Procleaner™ 110) for 10 min. AF1600 and Dursan coated sensors were cleaned by storing in 1% solution of Hellmanex™ in HPLC water for 30 min followed by storage in water for up to 2 h, thorough rinse with ethyl alcohol, and drying by nitrogen gas. These two sensor types were not exposed to sonication and UV/Ozone treatment as both methods were found to considerably lower the static contact angle of water on these surfaces transitioning them from hydrophobic to hydrophilic. AF1600 and Dursan coated sensors were treated with sonication at ultrasound frequency of ~42 kHz only when the effect of mechanical stress was intentionally evaluated. (*Caution: Adhering to the OSHA protocol for safe handling of potentially biohazardous material, upon completion of the experiments evaluating contact with normal human plasma proteins, all sensors and experiment modules were first treated by flowing 0.5% sodium hypochlorite solution in HPLC water.*)

The ratio of change in dissipation to change in frequency can be used to determine the rigidity of the adsorbed protein layer [7]. In case of detectable protein film formation, it was approximated that a rigid film had formed when $|\Delta D/\Delta f|$, at a given overtone, was $<0.1 \times 10^{-6}$ Hz^{-1}. Sauerbrey equation ($\Delta m = -C/n \cdot \Delta f$) correlating the adsorbed mass (Δm) to the changes in oscillation frequency (Δf) was used to differentiate adsorption of proteins on the surfaces [17]. In the equation, C is the mass sensitivity constant (with value of 17.7 ng cm^{-2} Hz^{-1} for the quartz sensors used here) and n is the overtone used for measurement. In case of protein films with $|\Delta D/\Delta f|$ values $>0.1 \times 10^{-6}$ Hz^{-1}, viscoelastic modeling using the Voigt model [18] was used to determine the adsorbed protein film properties. The Qtools software from Q-Sense allows calculation of both the Sauerbrey mass/thickness and viscoelastic properties using Voigt modeling. A minimum of two distinct measurements were carried out for each protein-surface system.

3. Results and discussion

3.1. XPS, SIMS analysis of the Dursan coating

Fig. 1 shows an XPS survey scan and SIMS depth profile of a representative Dursan coating on a stainless steel coupon to illustrate the atomic and bonding composition of the material. The combined XPS and SIMS data confirm that Dursan is composed of silicon, oxygen, carbon and hydrogen. The XPS scan in Fig. 1(a) represents the top 10 nm region of the coating, which includes both the surface functional layer as well as part of the bulk composition of the coating, but the surface functional layer contributes minimally to the bulk component. The XPS peaks below 200 eV are characteristic of silicon, and correspond to Si 3s (23 eV), Si 2p (100 eV) and Si 2s (149 eV), respectively. The peak at 281 eV is attributed to carbon 1s, and the strong peak located at 529 eV is characteristic of oxygen 1s. The peaks above the oxygen 1s peak are attributed to plasmon losses as well as Auger electron transitions generated during the XPS data collection.

In comparison to XPS, which studies the surface 10 nm region of the coating, SIMS depth profile was collected throughout the whole thickness of the representative coating (~730 nm). The uniform distribution of each component element (H, O, Si, and C) throughout the bulk of the coating is demonstrated in Fig. 1(b). The oxygen bump peaked near 800 nm into the coating indicates an oxide-rich interface between the coating and the stainless steel substrate. Based on RBS calibrated low-k standard, the Si:O atomic ratio is 1:2 (15.3% vs. 31%), suggesting the coating is comprised of a SiO_2-like bulk framework, with the remaining 10 atom% contribution from carbon and 43.7 atom% from hydrogen. The XPS study confirmed the same 1:2 Si:O ratio, with data generated by high resolution scans of each element and calibrated with the relative sensitivity factors of each element.

3.2. QCMD characterization

3.2.1. BSA adsorption

A wash buffer with surfactant is typically used in immunoassays for removal of unbound analytes [19,20] as well as for cleaning of different non-disposable immunoassay analyzer parts. To understand the effect of nonionic surfactant on protein adsorption to the Dursan coating and SS surface, WB1 (PBS buffer with a nonionic surfactant, Brij-35) was compared to WB2 (PBS buffer without the nonionic surfactant) and BSA was used as the model protein (Fig. 2). Both the baseline and rinse steps were obtained using respective buffers.

As shown in Fig. 2(a), upon exposure of the sensors to BSA solution, both the Dursan coated and bare SS sensors showed an instantaneous decrease in their resonance frequency indicating protein adsorption. The resonance frequency of a quartz crystal microbalance sensor decreases upon exposure of the sensor to a solution with higher density than that of the baseline buffer as well as a solution containing macromolecules such as proteins, polymers, or surfactants that can adsorb on the sensor surface [7]. The frequency drop for bare SS surface was 4-fold higher than that for Dursan coated surface. The sensors were then rinsed with WB1 (i.e. the buffer with nonionic surfactant), and a slight increase of frequency was observed for SS, whereas for Dursan the frequency reverted back to the baseline level. The dissipation increased instantaneously for both SS and Dursan upon contact with the protein solution indicating protein adsorption (Fig. 2(b)). Thereafter, in case of SS, a gradual increase in dissipation was observed until the sensor came in contact with the WB1 for the rinse, when the dissipation decreased slightly and plateaued over time to values above the baseline. In case of Dursan, the dissipation stayed relatively unchanged while in contact with the protein solution and decreased very close to the baseline values upon rinse with WB1. These observations indicated a much more effective removal of adsorbed BSA from the Dursan coated surface by the buffer containing nonionic surfactant than from the bare SS surface.

When WB2 (i.e. the buffer without surfactant) was used for baseline and rinse steps, an instantaneous decrease in frequency comparable to that of the buffer with surfactant (WB1) was observed for both SS and Dursan (Fig. 2(c)). Similarly, the dissipation increased for both SS and Dursan as the sensors came in contact with the protein solution (Fig. 2(d)). The decrease in frequency for SS was roughly 2-fold higher than that for Dursan. Further gradual decrease in frequency and increase in dissipation were observed for SS while it was in contact with the protein solution and until introduction of WB2 into the experiment chamber. Whereas, after the initial changes, the frequency and dissipation for Dursan stayed relatively unchanged until it came in contact with WB2 for the rinse step, when the frequency increased slightly in the beginning and stayed relatively unchanged over the next 20–25 min of the measurements for both SS and Dursan. The dissipation decreased in the beginning and stayed relatively unchanged over the rinse duration.

Thus, the presence of a nonionic surfactant, Brij-35 in the baseline/rinse buffer (i.e. WB1) at first led to comparatively lower adsorption, when 1% BSA was flowing over the Dursan coated surface, followed by near complete removal of the adsorbed protein upon rinse using WB1. On the other hand, the frequency difference between the rinse and baseline steps for Dursan shows that considerable amount of BSA was retained when a buffer without nonionic surfactant (WB2) was used. The nonionic surfactant in the buffer did not appear to impact adsorption or desorption of BSA on the bare SS surface as the frequency differences were comparable at rinse steps for both the WB1 and WB2 buffers.

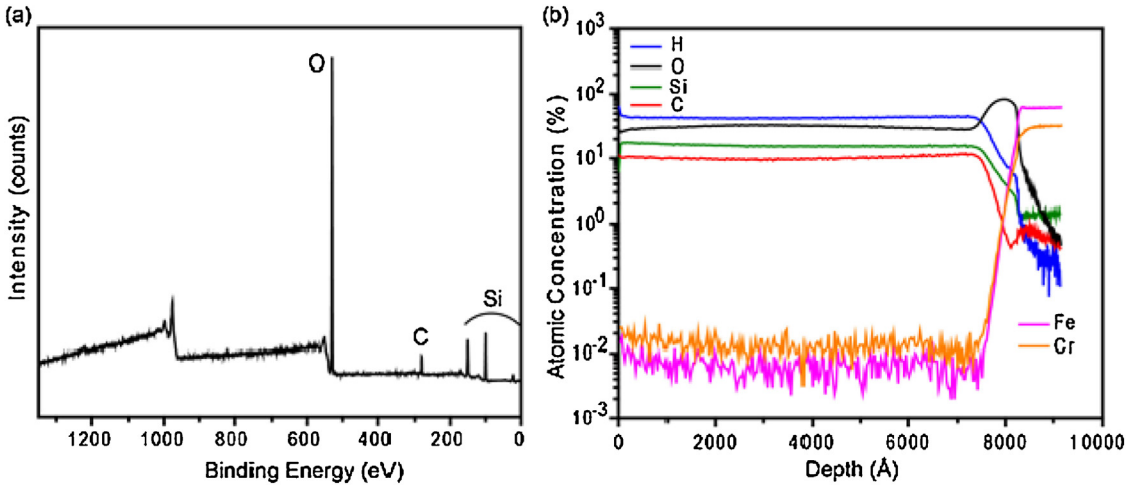

Fig. 1. XPS (a) and SIMS (b) spectra of a representative Dursan coating on a stainless steel coupon. In the SIMS spectra (b), the atomic percentages of elements H, O, Si and C are based on RBS calibrated low-*k* standard, whereas Fe and Cr (from the stainless steel substrate) are in arbitrary units (quantities not calibrated).

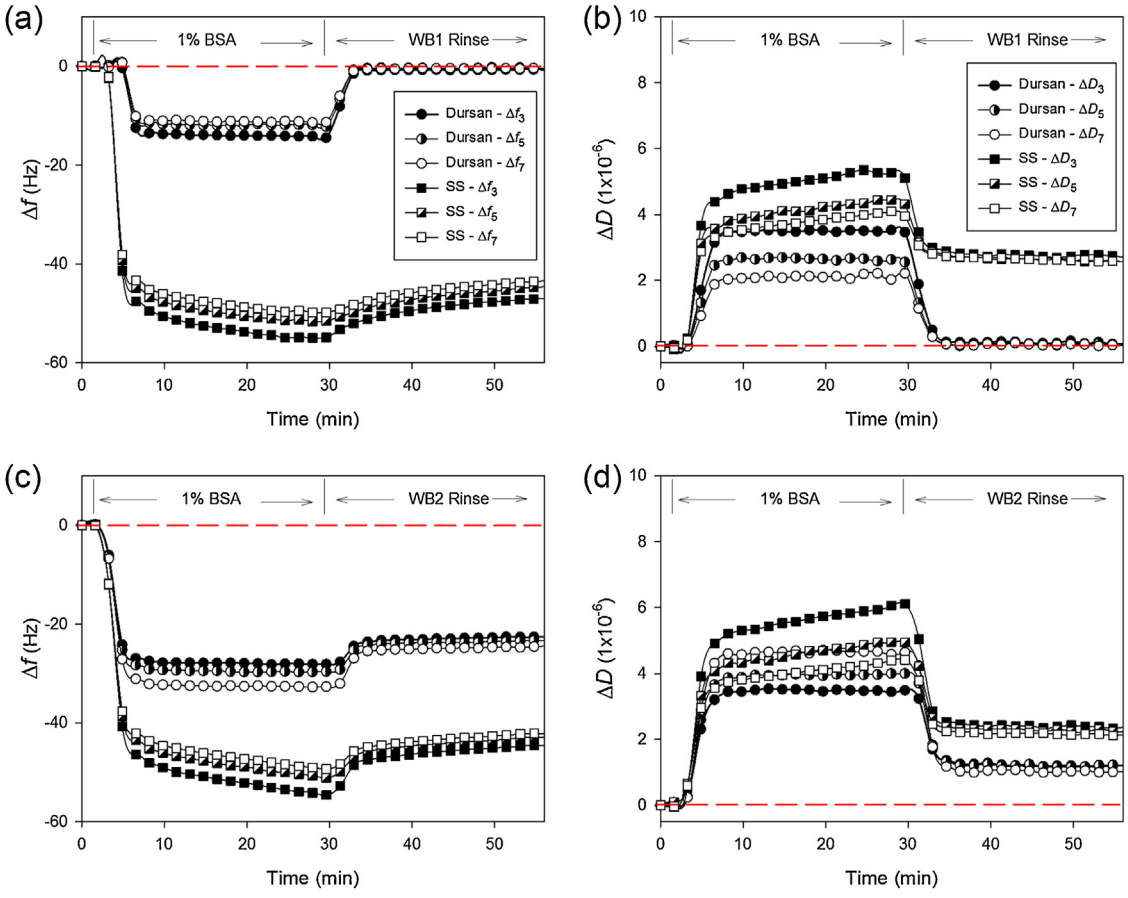

Fig. 2. Panels (a–d), respectively are the representative QCM-D profiles of sensor frequency (a), (c) and dissipation (b), (d) vs. time data at the 3rd, 5th, and 7th overtones comparing adsorption of BSA on Dursan coated and bare SS sensors. Wash buffers containing a nonionic surfactant (WB1) (panels (a) and (b)) and without surfactant (WB2) (panels (c) and (d)) as baseline and rinse solutions have been compared. Profiles in panels (c) and (d) follow the same symbol scheme as that of the profiles in panels (a) and (b). In these and the rest of the frequency and dissipation profiles, dashed red lines have been used to refer to the baseline values. Symbols have been used for visual guidance and also represent intermittant data points.

The observed changes in frequency for SS can be attributed to the adsorption of BSA on SS via electrostatic interactions bridged by a screening layer of monovalent metal ions (Na^+) [21] between predominantly negatively charged BSA [22] and negatively charged 316L grade SS QCM-D sensor [16] at pH 7.2. Adsoprtion is also presumed to be assisted by nanostructural surface irregularities [15] as well as hydrogen bonding interactions [23]. Some structural rearrangement of the protein molecules at the sensor surface caused the gradual decrease in frequency when the latter was in contact with the protein solution prior to the rinse. As was observed by Marsh et al. [24] in studies evaluating displacement of β-lactoglobulin from hydrophilic silica surface by

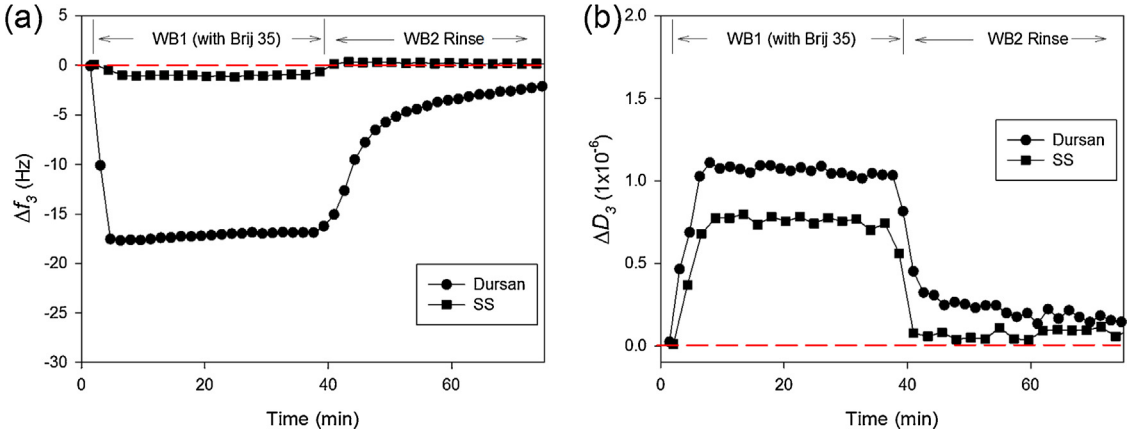

Fig. 3. Panels (a) and (b), respectively are the representative QCM-D profiles of sensor frequency and dissipation vs. time data at the 3rd overtone comparing adsorption of Brij-35 on Dursan coated and bare SS sensors. Wash buffer without Brij-35 (WB2) was used for the baseline and rinse steps, whereas the buffer containing Brij-35 (WB1) was used as sample.

nonionic octaethylene glycol monododecyl ether ($C_{12}E_8$) surfactant, the presence of a nonionic surfactant in the baseline/rinse buffer in our study also did not impact adsorption of a globular protein (BSA) on hydrophilic SS surface. On the other hand, in case of the hydrophobic Dursan surface, our observations with WB2 (the buffer without surfactant) for baseline/rinse steps show that BSA adsorption was driven primarily by the hydrophobic interactions that have been reported to facilitate adsorption of globular proteins to hydrophobic surfaces [23,25,26]. When WB1 was studied as a sample using WB2 for baseline and rinse steps, we found that a considerable amount (~40 ng cm^{-2}) of Brij-35 was adsorbed on Dursan and no detectable amount of Brij-35 was adsorbed on SS (Fig. 3). Based on these observations, we have hypothesized a 2-way adsorption mechanism in which (a) Brij-35 first formed a layer of surfactant on hydrophobic Dursan (during the baseline step) exposing its hydrophilic polyoxyethylene domains to BSA molecules, thus allowing comparatively lower BSA adsorption on Dursan through weaker van der Waal's interactions, and (b) then displaced the adsorbed BSA from the solid-liquid interface by significantly weakening those interactions during the rinse step. Thus the pre-adsorbed Brij-35 on Dursan during the protein exposure step might have worked similarly to the PEG based hydrophilic but uncharged polymeric films that have been reported to reduce adsorption of globular proteins [2,4,5]. During the rinse step, Brij-35 acted same as the nonionic surfactants displacing globular proteins adsorbed at hydrophobic interfaces [24,27,28]. The differences in density and viscosity of the BSA solution vs. WB1 could also have contributed to the observed changes in frequency and dissipation of the Dursan coated sensor prior to the rinse using WB1. However, the magnitudes of change, $|\Delta f| \approx 10$ Hz and $|\Delta D| \approx 2$ units, tilt the scale more towards the hydrophilic interactions of BSA molecules with the in-situ Brij-35 film. The Dursan surface is made up of alkyl functional groups (with water contact angle of ~90°) and therefore the protein adsorption on Dursan via the electrostatic interactions can be ruled out.

The absolute ratio of the change in dissipation to the change in frequency, i.e. $|\Delta D/\Delta f|$ as well as separation between the overtones were used to discriminate between the rigid and viscoelastic characteristics of the adsorbed protein layers [7,18,29]. As shown in Table 1, $|\Delta D/\Delta f|$ was $<0.1 \times 10^{-6}$ Hz^{-1} for BSA adsorbed on SS, whereas there was negligible retention of protein on Dursan coating after WB1 rinse. Hence, as a qualitative comparison measure, along with the change in frequency at the 3rd overtone, Sauerbrey mass was used to differentiate adsorbed amounts of BSA on these two surfaces. Adsorbed BSA amount on SS of ~760 ng cm^{-2} using the Sauerbrey equation was slightly higher than the value of 610 ng cm^{-2} reported by Gispert et al. [30] for adsorption of BSA at similar solution concentrations on 316L grade stainless steel QCM-D sensor, and closer to the maximum surface coverage of 720 ng cm^{-2} estimated by Wertz and Santore [26] for a closely-packed monolayer of BSA molecules in end-on orientation on a hydrophobic surface. The maximum surface coverage of 720 ng cm^{-2} estimated by Wertz and Santore [26] would result in a film thickness of ~6 nm using hydrated protein film density of 1200 g cm^{-3} [31] and appears to be an underestimation for a protein film with end-on molecular orientation if the authors' reported BSA dimensions of $4 \times 4 \times 14$ nm^3 were considered. In our study, the Sauerbrey thickness of the BSA layer on SS was determined to be ~6.4 nm using the protein film density of 1200 g cm^{-3}. For the film thickness discussion, it would be appropriate to consider the advances in which previously assumed elongated ellipsoidal structure of BSA molecule resulting in dimensions of $4 \times 4 \times 14$ nm^3 was corrected to crystallographically determined heart-shaped [32–34] with dimensions of $8 \times 6.9 \times 3$ nm^3 [32,35]. The Sauerbrey thickness in our study falls within the dimensions reported for both the elongated ellipsoidal and heart-shaped structures of serum albumins. As specified earlier, besides the dry protein mass, the measurements using QCM-D can also detect hydration of protein films on hydrophilic surfaces [29,36]. Hence, the adsorbed mass and thickness of BSA film on SS in our study are certainly due to mixed (both end-on and side-on) orientations of BSA molecules. In addition to the only monovalent cation (Na^+) that we have used in our study, the buffer system used by Gispert et al. included divalent cations such as Ca^{2+} and Mg^{2+} [30]. Multivalent cations have been shown to suppress electrostatic repulsion between negatively charged BSA molecules [37]. This suppression of electrostatic repulsion at solution pH above the isoelectric point (p*I*) of BSA (ca. 4.6) could explain formation of more compact BSA films with comparatively lower Sauerbrey adsorbed mass in studies by Gispert et al.

$|\Delta D/\Delta f|$ was $<0.1 \times 10^{-6}$ Hz^{-1} for BSA adsorbed on SS. However, the frequency overtones at the rinse step were separated (Fig. 2(a)). Hence, viscoelastic modeling of the frequency and dissipation data was conducted using Voigt model. (Please refer to Supplementary Information Fig. S-F1(a) for the fitted data profiles and Table S-T1 for parameters used in viscoelastic modeling.) The modeled BSA mass of ~880 ng cm^{-2} was greater than the Sauerbrey mass calculated assuming a rigid protein film, confirming hydration of the adsorbed protein film. The modeled thickness of the BSA layer was determined to be ~8.4 nm, which was slightly higher than the longest reported dimension of the heart-shaped albumin molecule [32,35].

Table 1
QCM-D data for the studied protein-surface systems. Mean (±SD) values of the 3rd overtone data with normalized frequency changes have been reported.

Coating	Δf_3 (Hz)		ΔD_3 (1×10^{-6})		$\lvert\Delta D_3/\Delta f_3\rvert$ (10^{-6} Hz^{-1})		Sauerbrey mass (ng/cm^2)		Sauerbrey thickness (nm)		Viscoelastic mass (ng/cm^2)	Viscoelastic thickness (nm)
	Dursan	SS	Dursan	SS	Dursan	SS	Dursan	SS	Dursan	SS	SS	SS
Protein w/buffer												
BSA w/WB1	0.06$^{(5)}$ (±0.9)	−43.74$^{(4)}$ (±6.9)	0.37 (±0.4)	2.33 (±0.6)	1.95*	0.05	−1.1 (±15)	767(±122)	0.00 (±0.1)	6.4 (±1.1)	883(±168)	8.4 (±1.6)
Mouse IgG w/WB1	−4.00$^{(2)}$ (±0.7)	−90.40$^{(2)}$ (±1.3)	0.46 (±0.2)	5.69 (±0.1)	0.12*	0.06	70.1 (±12.9)	1586(±23)	0.6 (±0.1)	14.4 (±0.2)	1851(±8)	17.6 (±0.1)
BSA w/WB2	−22.90$^{(4)}$ (±2.6)	−47.50$^{(3)}$ (±1.7)	1.83 (±0.8)	2.50 (±0.1)	0.08	0.05	489(±45)	834(±29)	4.1 (±0.4)	6.9 (±0.2)	969(±10)	9.2 (±0.1)

$^{(x)}$ represents number of measurements for a given protein-coating system.
* Although, $\lvert\Delta D_3/\Delta f_3\rvert$ values for Dursan coating are >0.1×10^{-6} Hz^{-1}, due to near zero frequency at rinse step, Sauerbrey equation was used to calculate the hypothetical surface mass and thickness of the adsorbed protein.

For BSA adsorbed on SS in presence of WB2 for baseline/rinse, the Sauerbrey mass and thickness, respectively were ~820 ng cm^{-2} and ~6.9 nm, and the viscoelastic mass and thickness obtained using Voigt model were ~960 ng cm^{-2} and ~9.2 nm. These values for the BSA/WB2 system were statistically comparable to corresponding mass and thickness values obtained the for BSA/WB1 system, indicating negligible effect of the non-ionic surfactant, Brij-35 in the baseline/rinse buffer on adsorption of BSA on hydrophilic SS surface. (Please refer to Supplementary Information Fig. S-F1(b) for the fitted data profiles and Table S-T1 for parameters used in viscoelastic modeling.) The modeled BSA mass in our study was statistically closer to that of 1100 ng cm^{-2} reported by Jin et al. [25] for viscoelastic films of BSA on hydrophilic monomethoxy poly(ethylene glycol) surface.

Although the $\lvert\Delta D/\Delta f\rvert$ value was >0.1×10^{-6} Hz^{-1} for BSA adsorbed on Dursan coated sensor with WB1 for baseline/rinse, since there was negligible retention of protein on the surface (Δf = ~0 Hz), the $\lvert\Delta D/\Delta f\rvert$ ratio was deemed immaterial. In case of BSA adsorbed on Dursan with WB2 (i.e. PBS w/o surfactant) for baseline/rinse, $\lvert\Delta D/\Delta f\rvert$ was ca. 0.04×10^{-6} (or <0.1×10^{-6}) Hz^{-1} and the Sauerbrey mass and thickness calculated assuming rigid protein film were ~490 ng cm^{-2} and ~4.1 nm. Extended viscoelstic modeling, which utilizes frequency based layer 1 viscosity and shear parameters in conjunction with the other modeling parameters of the Voigt model, was employed to model the frequency and dissipation data for BSA/WB2 system on Dursan (Fig. S-F1(c) and Table S-T1). Modeled mass and thickness were determined to be ~570 ng cm^{-2} and ~5.4 nm. Adsorbed BSA mass on hydrophobic surfaces can vary with the surface type. Formation of BSA multilayers (as interpreted by the authors through nearly 1200 ng cm^{-2} of adsorbed mass) has been reported by Jin et al. [25] on hydrophobic poly(ethylene-co-acrylic acid) films. The Sauerbrey and modeled thickness of the BSA adsorbed on Dursan (with WB2) in our study are between the 2nd and 3rd largest dimensions of the heart-shaped albumin molecule [32,35] alluding to the mixed side-on and end-on orientations of adsorbed BSA molecules on the Dursan coating.

Nevertheless, the statistically significant differences in the resonance frequencies at the 3rd overtone as well as the differences in the adsorbed protein mass (obtained using Sauerbrey equation and the viscoelastic modeling) demonstrated that the Dursan coating was effective in complete prevention of non specific adsorption of BSA in the presence of non-ionic surfactant Brij-35.

3.2.2. *Mouse IgG adsorption*

Mouse IgG showed adsorption behavior similar to that of BSA on Dursan and SS surfaces when WB1 buffer was used. A considerable decrease in frequency (Fig. 4(a)) and increase in dissipation (Fig. 4(b)) were observed for SS within a few minutes of exposure to the protein solution. The corresponding changes on Dursan were relatively slower (by ~8–10 min). A gradual decrease in frequency and increase in dissipation occurred for both SS and Dursan during contact with the protein solution. The frequency increased back by about 20% for SS upon introduction of WB1 into the experimental chamber, still resulting in considerable retention of mouse IgG on SS. In the case of Dursan, the frequency reverted back closer to the baseline value upon the introduction of WB1, resulting in negligible retention of adsorbed mouse IgG on the Dursan coating. Considerable dissipation shift was observed in case of SS during the WB1 rinse, whereas, the dissipation reverted back closer to the baseline values in case of Dursan.

Similarly to that of BSA adsorption, three different events cumulatively could be driving the observed changes in frequency for mouse IgG adsorbing on SS: (i) electrostatic interactions bridged by a screening layer of monovalent metal ions (Na^+) [21] between slightly negatively charged mouse IgG (pI = ~7.0) and negatively

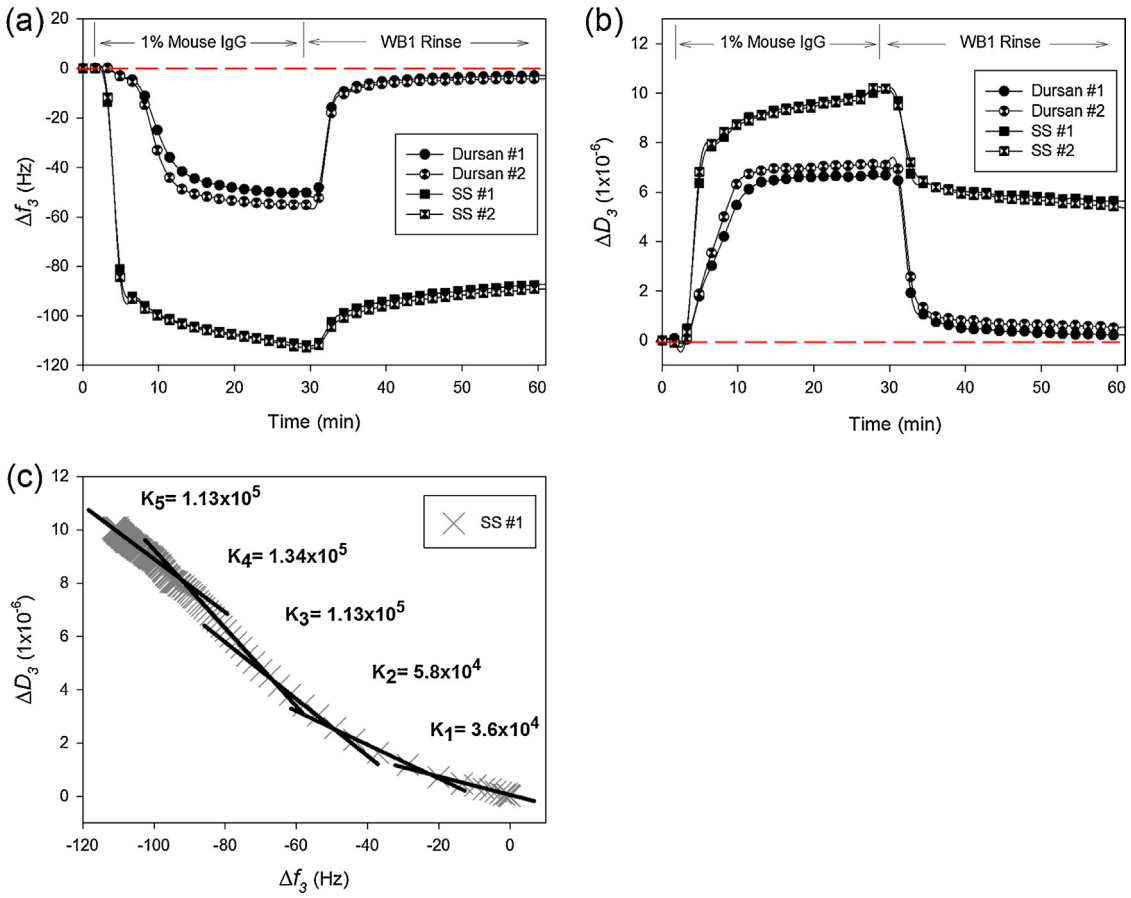

Fig. 4. Panels (a) and (b), respectively are the representative QCM-D profiles of the sensor frequency and dissipation vs. time at the 3rd overtone comparing adsorption of Mouse IgG on two different Dursan coated and two bare SS sensors. Wash buffer with Brij-35 (WB1) was used for the baseline and rinse steps. Panel (c) is the ΔD vs. Δf profile generated from the experimental data prior to the rinse step of mouse IgG adsorption on bare SS (#1) surface. Five distinct slopes were established.

charged 316L grade SS QCM-D sensor [16] at pH 7.2; (ii) adsorption due to nanostructural surface irregularities; as well as (iii) adsorption due to the hydrogen bonding interactions of protein molecules with the charged interface. (Note: The isoelectric point (p*I*) of mouse IgG was determined using capillary isoelectric focussing (CIEF).) The gradual decrease in frequency when the sensors were in contact with the protein solution can be attributed to the structural rearrangement of the protein molecules at the solid-liquid interface. For IgG adsorbed on SS, $|\Delta D/\Delta f|$ was $<0.1 \times 10^{-6}$ Hz^{-1}. Although the ratio was $>0.1 \times 10^{-6}$ Hz^{-1} for Dursan, it can be considered insignificant for comparison purposes as there was very low protein adsorption. The Sauerbrey mass of IgG adsorbed on SS was ~1580 ng cm^{-2}. The average adsorbed IgG mass was determined to be ~1840 ng cm^{-2} using the Voigt model for the viscoelastic films (Fig. S-F1(d) and Table S-T1). In comparison, very low amount of IgG was adsorbed on Dursan (~70 ng cm^{-2} – calculated using both the Sauerbrey equation and Voigt models). Adsorbed IgG amount on SS in this study is considerably larger than the reported amounts of immunoglobulins electrostatically adsorbed on hydrophilic surfaces such as titanium dioxide, mica, aminopropyl (triethoxysilane) modified silicon dioxide [38–40], and the amounts of ~550 ng cm^{-2} that can theoretically be obtained for a densely packed intact IgG monolayer with protein molecules adsorbed in end-on orientation [41,42]. The observed higher mass of IgG in our study can be attributed to the capability of QCM-D measurements to record the coupled water content in adsorbed protein layer [29,36,38] vs. other methods detecting dry protein mass [39,40], to the different type of hydrophilic surfaces studied, and plausibly to the general tendency of IgG to form multilayers on stainless steel as well as on hydrophobic surfaces above certain bulk IgG concentrations [43,44]. Fig. 4(c) shows the ΔD_3 vs. Δf_3 plot of the experimental data obtained for adsorption of mouse IgG on bare SS sensor surface prior to the rinse step. Different slopes in this type of plot indicate different kinetic processes of protein adsorption [44,45] when the bulk protein solution is in contact with the sensor. Zhou et al. [44] have reported establishment of multiple slopes for IgG adsorbed on hydrophobic surfaces at bulk concentrations above 57.5 μg/mL (or 0.00575%, w/v). Multiple slopes were also established in our study with mouse IgG adsorbed at a bulk concentration of 1% (w/v) and the slopes at higher frequency/dissipation values (K_3, K_4 and K_5) were almost an order of magnitude higher than the slope at the beginning stages of the experiment run (K_1). Slope K_1 represents protein adsorption and formation of a compact monolayer, whereas slopes K_3–K_5 represent loosely bound multilayer. This multilayer however appears to be more or less completely removed during the rinse step, for, as shown in Table 1, the Sauerbrey as well as Voigt modeled thicknesses of 14.4 and 17.6 nm, respectively of the adsorbed mouse IgG at the rinse step are in the vicinity of the longest structural dimension of an IgG molecule [46,47]. Since QCM-D measurements do take into consideration the hydration of the adsorbed protein film and random adsorption of protein molecules would occur at the high bulk concentrations used in our study, the adsorbed IgG layer is presumed to be a mixture of both the side-on and end-on orientated molecules.

Immunoglobulins also adsorb on hydrophobic surfaces such as polystyrene [41,42], Teflon-amorphous fluoropolymer (Teflon-AF) [38], and 1-octadecanethiol modified gold [44] via hydrophobic interactions. However, as was observed in the case of BSA (Section

3.2.1), the presence of a nonionic surfactant, Brij-35, in the baseline/rinse buffer in our study significantly reduced or prevented IgG adsorption on the hydrophobic Dursan surface.

3.2.3. Effect of chemical and sonication cleaning on coating performance

Treatment by sodium hypochlorite solutions [48,49], alkaline solutions with surfactants [50,51] and sonication [50,52,53] are few of the effective surface cleaning methods employed in various industries. As described in this paper's experimental methods section, bare SS and Dursan and AF1600 coated sensors, when they were used to study adsorption of proteins from potentially biohazardous normal human plasma (NHP), were exposed to flow of 0.5% sodium hypochlorite for 30 min followed by cleaning using flow of 2% Hellmanex for 30 min, followed by flow of HPLC water for 2 h. In a separate set of experiments, the sensors were also exposed to 10 min of sonication in ethanol to evaluate the effect of mechanical wear in polymeric coatings [54,55] on protein adsorption. The SS sensor was used as a control. Water contact angle of the sensor dried under nitrogen stream was measured to evaluate effect of harsh chemical exposure and sonication-induced mechanical wear. Optical microscopy was used to determine degree of mechanical wear.

A considerable gradual decrease in water contact angle was observed for Dursan exposed to the multiple harsh chemical cleanings post QCM-D experiments turning the sensor hydrophilic (with an average water contact angle of $54 \pm 9^\circ$ across 9 different sensors). Changes in water contact angle of a representative Dursan and AF1600 coated sensor after a given treatment step are shown in Table 2. Subsequent sonication of the Dursan coated sensor in ethanol did not appear to alter the water contact angle changed due to chemical exposure. On the other hand, the contact angle of the AF1600 coated sensor did not undergo any considerable changes upon cleaning post QCM-D experiments ($120 \pm 6^\circ$), but dropped considerably to $50 \pm 11^\circ$ upon sonication turning the sensor surface hydrophilic. Additionally, when the treated Dursan coated sensors were briefly sonicated in deionized water for 40 seconds, the average contact angle increased ~14% to $61 \pm 10^\circ$. This indicates a reversible and/or semi-reversible influence from the test and cleaning solutions as they interact with the Dursan surface, whether it be adsorption and/or oxidation. Conversely, for the AF1600 surface, the similar decrease in hydrophobicity (~120° to ~50°) after ethanol sonication was not altered by extensive (10 min) ethanol sonication and subsequent water rinsing. Exposure to oxidizing conditions such as ozone treatment or use of harsh chemicals have been reported to induce hydrophilicity in the hydrophobic self-assembled monolayers of alkylsilane molecules on different substrates [56,57]. Polymer films of polyethylene and poly(tetrafluoroethylene-co-hexafluropropylene) – a fluoropolymer – have also been reported to undergo hydrophobic to hydrophilic change upon oxidation induced by harsh chemicals [58]. Thus the change in water contact angle of the Dursan coated sensor in our study can be attributed to the exposure to the harsh chemicals. Although, the decrease in contact angle of AF1600 coated sensor upon sonication is intriguing.

Table 2
Changes in water contact angle of a representative unit of a coated sensor after a given treatment.

Coating	Dursan	AF1600
Treatment		
None	~90°	~120°
2% HM (1×) + water	~72°	~120°
0.5% NaOCl + 2% HM (2×) + water	~43°	~120°
0.5% NaOCl + 2% HM (2×) + water + sonication in ethanol	~45°	~50°

AF1600 coating was deposited on gold sensor using a proprietary solvent based spin-coating technique by Biolin Scientific, Inc. Senda et al. [59] have reported that the substrate adhesion strength of fluoropolymer thin films, deposited using conventional organic solvent based wet processes, was poorer than ion-assisted vapor deposition polymerization method. In our study, upon sonication, no visible changes were detected in Dursan coating, which was deposited using a chemical vapor deposition method on a SS QCM-D sensor (Fig. 5(a and b)), whereas some delamination of the spin-coated fluoropolymer AF1600 coating from the substrate was observed (Fig. 5(c and d)). Multiple sensors of each coating were sonicated. All of the cleaned and sonicated Dursan coated sensors did not show any significant contact angle change between cleaning and sonication, whereas all of the sonicated AF1600 coated sensors showed considerable decrease from ~120° to ~50°. Coating delamination was observed in only a few of the sonicated AF1600 coated sensors.

For protein adsorption studies, treated (i.e. cleaned and sonicated) Dursan and AF1600 coated sensors without any visible delamination post-sonication were exposed to normal human plasma (a representative of patient samples utilized in diagnostics analyzers) with WB1 (i.e. the buffer with Brij-35) as baseline/rinse buffer. Proteins in normal human plasma consist of 3.5–5% by weight of serum albumins, up to 2.5% by weight of different immunoglobulins, and varying low concentrations of multiple other proteins [14]. Overall protein content in human plasma can be as high as 8%. We have seen in Sections 3.2.1 and 3.2.2 that many of the plasma proteins (mainly albumins and immunoglobulins) would adsorb on Dursan coating if a wash buffer without a surfactant (or WB2) was used, and would not adsorb if wash buffer with nonionic Brij-35 (or WB1) was used as baseline/rinse buffer. Similarly, as shown in Fig. 5(e and f), nearly zero frequency and dissipation changes at the rinse steps meant that, even with the considerably high protein content in the human plasma, none of the plasma proteins were retained on the untreated Dursan and AF1600 sensors, as well as the treated Dursan sensor. Negative frequency and positive dissipation at the rinse meant that a considerable amount of plasma proteins was retained on the sonicated AF1600 sensor, indirectly pointing toward loss of protein resistant properties of the hydrophobic AF1600 coating post-sonication. Although the Dursan coating turned hydrophilic upon cleaning by harsh chemicals, it retained its protein resistant characteristics. Thus, hydrophobicity could not be the only determinant of differential adsorption behavior of plasma proteins on the treated Dursan vs. AF1600 coatings and the microscopic structure of the surface as well as deformities developed upon sonication could be playing a significant role. A verification run was performed in which two units of the treated (i.e. cleaned and sonicated) Dursan and AF1600 coated sensors were exposed to NHP proteins using WB2 (buffer w/o Brij-35) as the baseline/rinse buffer. A comparison of the obtained frequency profiles to those obtained using WB1 (buffer w/Brij-35) confirmed that Brij-35 was indeed required for the Dursan surface to maintain its protein-resistant properties (Fig. 5(g)). Whereas, irrespective of the baseline/rinse buffer used, a comparable adsorption of plasma proteins occurred on the treated AF1600 sensor, confirming loss of its protein resistant properties upon sonication. A considerable amount of plasma proteins was adsorbed and retained on the SS surface (see Fig. S-F2 and Table 3). As majority of the plasma proteins are albumins and immunoglobulins, the electrostatic interactions of predominantly negatively charged proteins through salt ion bridging with negatively charged stainless steel caused the proteins to permanently adsorb on SS surface. Sauerbrey mass and thickness of the NHP proteins adsorbed on SS were roughly 20% higher than that of BSA and roughly 50% lower than that of mouse IgG. It can be corroborated that the majority of the adsorbed NHP proteins on SS were albumins. The modeled mass

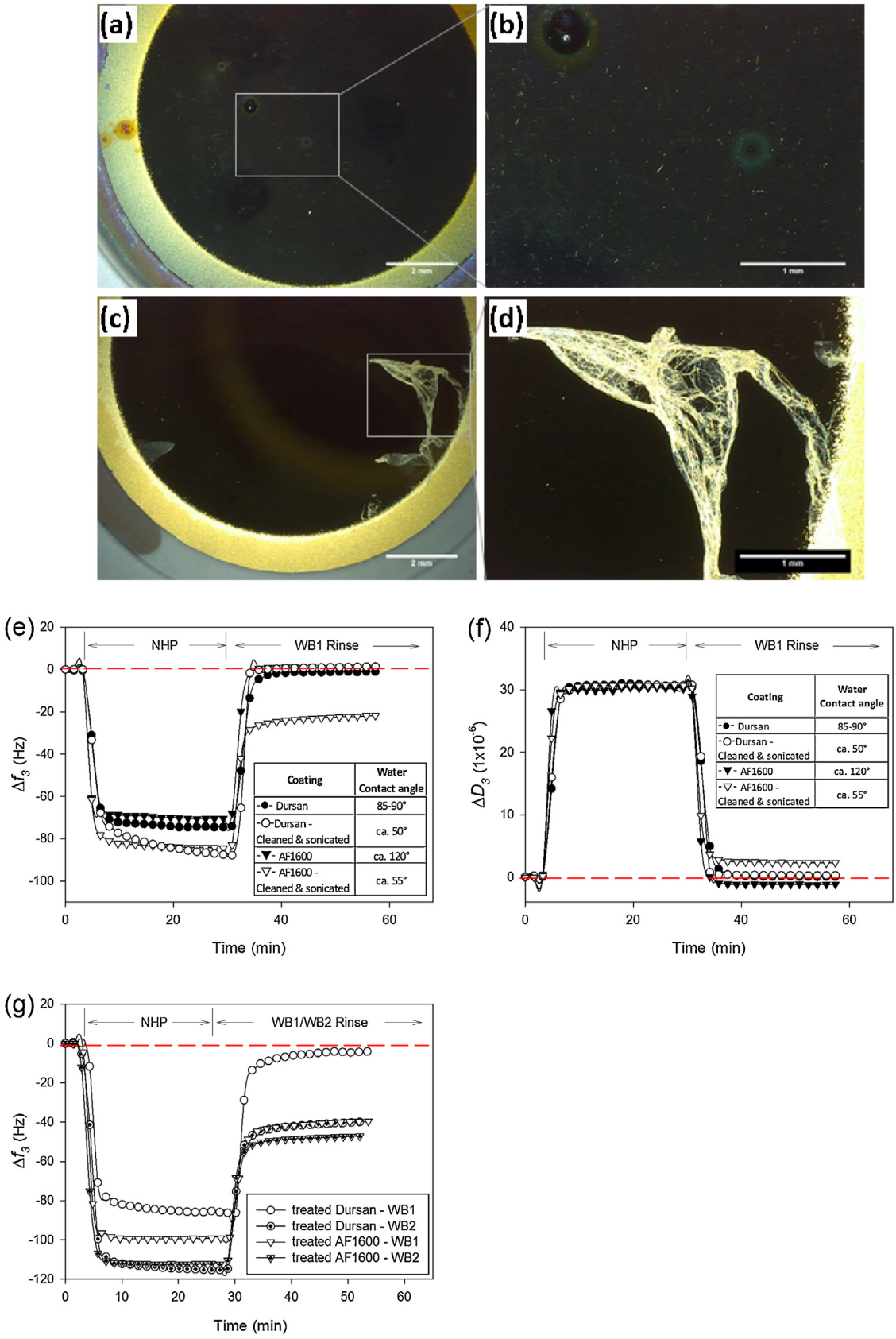

Fig. 5. Panels (a)–(d) are the representative optical micrographs of the QCM-D sensors showing intact Dursan coating ((a) and (b)) and coating delamination of AF1600 coating ((c) and (d)) taken at 30× ((a) and (c)) and 100× ((b) and (d)) optical magnifications, respectively. Panels (e) and (f), respectively are the representative QCM-D profiles of sensor frequency and dissipation vs. time at the 3rd overtone comparing adsorption of normal human plasma (NHP) proteins on treated (i.e. cleaned and sonicated) vs. untreated Dursan and AF1600 coatings. Wash buffer with Brij-35 (WB1) was used for the baseline and rinse steps. Panel (g) shows frequency profiles comparing adsorption of NHP proteins on treated Dursan and AF1600 coated sensors when either WB1 (w/Brij-35) or WB2 (w/o Brij-35) was used as the baseline/rinse buffer.

Table 3
QCM-D data for the studied normal human plasma (NHP) protein-surface system with WB1 as baseline/rinse buffer. Mean (±SD) values of the 3rd overtone data with normalized frequency changes have been reported.

	Δf_3 (Hz)			ΔD_3 (1×10^{-6})			$\lvert\Delta D_3/\Delta f_3\rvert$ (10^{-6} Hz^{-1})			Sauerbrey mass (ng/cm^2)			Sauerbrey thickness (nm)	Viscoelastic mass (ng/cm^2)	Viscoelastic thickness (nm)
Coating	Dursan	SS	AF1600	Dursan	SS	AF1600	Dursan	SS	AF1600	Dursan	SS	AF1600	SS	SS	SS
Protein															
Prior to surface cleaning and sonication (for Dursan) and prior to sonication (for AF1600). Regular cleaning of SS was followed. Hence, only the post cleaning/sonication data are reported below for SS.															
NHP	−0.7[3] (±0.9)	–	1.0[2] (±0.1)	0.2 (±0.3)	–	−0.2 (±1.3)	n/a	–	n/a	13 (±16)	–	n/a*	–	–	–
Post surface cleaning and sonication (for all)															
NHP	−1.6[11] (±2.6)	−57.2[4] (±0.3)	−30.0[5] (±12.1)	0.1 (±0.3)	3.8 (±0.2)	2.4 (±0.0)	0.06	0.07	0.08	28 (±46)	1024 (±4)	526** (±213)	8.8 (±0.5)	1190 (±46)	10.5 (±1.5)

(x) number in parantheses represents number of measurements for a given protein-coating system.
* Sauerbrey mass was not calculated due to positive frequency for AF1600 pre-sonication.
** Viscoelastic modeling was not performed for the AF1600 data.

and thickness for NHP proteins adsorbed on SS (obtained using Voigt modeling of the frequency and dissipation data) were roughly 20% higher than the corresponding Sauerbrey values giving due consideration to the hydration of the adsorbed protein film. (Please refer to Fig. S-F2(c) and S-T1 for data fit and model parameters.)

3.2.4. *Poly-L-lysine adsorption*

The protein-resistant property of the Dursan coating was challenged by studying adsorption of a synthetic amino-acid polymer poly-L-lysine (PLL; mw ~9000), which exhibits a positive charge at neutral pH and is used extensively for patterning cell culture substrates [13]. It is one of the polycations typically used in diagnostics reagent formulations to prevent assay interference from the red blood cells in a patient sample [60]. We studied PLL adsorption on bare SS and Dursan coated sensors at different bulk concentrations. Changes in frequency and dissipation vs. time are shown in Fig. 6. A concentration dependent adsorption behavior was observed on Dursan. The frequency gradually increased during contact with the 0.1% and 0.25% PLL solutions and, after roughly 20 min of contact with the protein solution, reached a plateau for 0.1% PLL and a maximum followed by slight decrease for 0.25% PLL solution (Fig. 6(a)). This behavior of PLL solution is exactly opposite of the observations with BSA and Mouse IgG. The densities and viscosities of WB1 (buffer with surfactant), 0.1% PLL and 0.25% PLL solutions were comparable (density = ca. 1.007 g/mL and viscosity = ca. 0.93 cP at 100 s^{-1} shear rate). The upward shift in the frequency was not observed when the buffer without surfactant (WB2) was used as baseline/rinse buffer and some PLL adsorption was also detected (Fig. 6(c)). Hence, the upward shift in sensor frequency during contact with the 0.1% and 0.25% PLL solutions with WB1 suggests that the Brij-35 surfactant molecules, adsorbed during the baseline flow, were being displaced from the Dursan surface by PLL. During the WB1 rinse step, the frequency instantaneously decreased to values closer to the baseline, indicating negligible adsorption of PLL on Dursan from solutions with 0.25% or lower PLL concentration. This phenomenon of displacement of Brij-35 by PLL from Dursan has been demonstrated in Fig. 6(d), in which (i) baseline was generated using WB2, followed by (ii) WB1 (buffer with Brij-35) flow over the sensors, followed by (iii) exposing the sensors to 0.1% PLL solution, and finally (iv) rinsing the sensors using WB2. The comparable frequency values (~0 Hz) between the rinse and baseline steps confirmed our observations in Fig. 6(a) that exposing the Dursan surface to PLL displaced the preadsorbed Brij-35 molecules.

In case of 1% PLL, the frequency first decreased for few minutes followed by a gradual increase to values closer to the baseline (Fig. 6(a)). After nearly 10 min of exposure of the sensor to the 1% solution, the frequency decreased gradually until introduction of the WB1. We think that this *S*-shaped behavior of the 1% PLL solution during contact with Dursan surface indicates three successive events: (i) the decrease in frequency due to adsorption of PLL from a concentrated solution on pre-adsorbed Brij-35 (from the baseline), followed by (ii) the comparable increase in frequency due to near complete removal of pre-adsorbed Brij-35 by PLL, and (iii) the subsequent adsorption of PLL due to the increased interfacial ordering of polymer backbones of the densely charged PLL molecules at the hydrophobic interface [61]. The frequency did not revert back to the baseline values during the WB1 rinse. Thus, considerable amount of PLL was retained on the Dursan surface in case of 1% PLL solution. On SS, for all of the evaluated PLL concentrations, the frequency decreased as soon as the sensor came in contact with the PLL solution and stayed relatively unchanged until introduction of the WB1. During the WB1 rinse, the frequency increased initially and reached a plateau after few minutes. Nearly overlapping 3rd overtone profiles during WB1 rinse for the studied PLL concentrations indicate that a monolayer of PLL was formed on SS

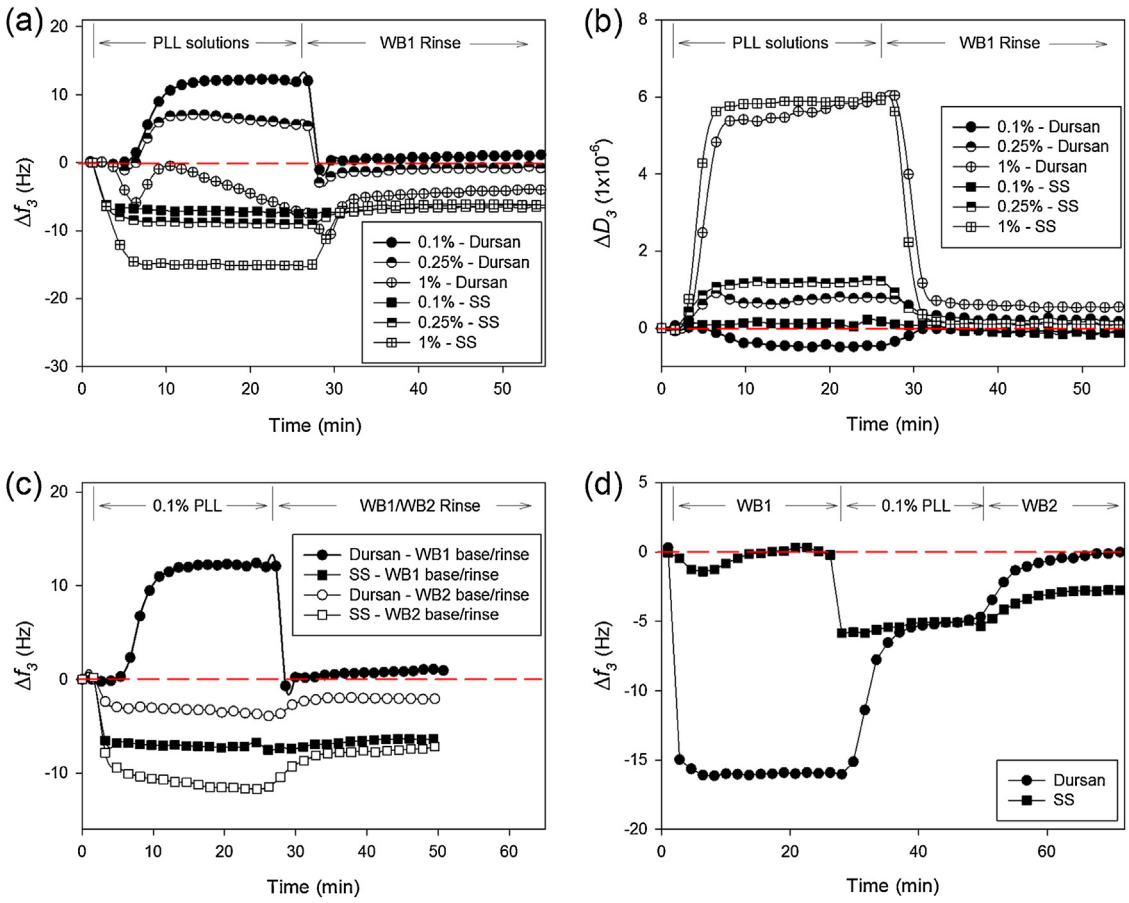

Fig. 6. Panels (a) and (b), respectively are representative QCM-D profiles of sensor frequency and dissipation vs. time at the 3rd overtone comparing adsorption of poly-L-lysine (PLL) at different solution concentrations on Dursan coated and bare SS sensors. Wash buffer with Brij-35 (WB1) was used for the baseline and rinse steps. Panel (c) shows frequency profiles comparing adsorption of PLL from a 0.1% solution on Dursan coated and bare SS sensors with either WB1 or WB2 as baseline and rinse solution. Panel (d) shows frequency profiles at the 3rd overtone demonstrating displacement of Brij-35 by PLL from the Dursan coated sensor surface.

surface at neutral solution pH. For any given PLL concentration, the absence of enough separation between the overtones during the rinse step did not allow appropriate viscoelastic modeling of the experimental data (Fig. S-F3).

The dissipation showed opposing trends between 0.1% and 0.25% solutions in case of PLL adsorption on Dursan coated sensor with WB1 as baseline/rinse buffer (Fig. 6(b)). It gradually decreased to about -0.5×10^{-6} units upon contact of the sensor with 0.1% PLL solution, stayed relatively unchanged until the rinse, and reverted back to the baseline values during the rinse. For 0.25% PLL, it increased initially to about 0.6×10^{-6} units during contact with the sensor, stayed relatively unchanged thereafter, and decreased closer to the baseline values upon rinse. The opposite directions of the frequency and dissipation profiles for 0.1% PLL solution are in good agreement with the typical trends of QCM-D profiles for macromolecular interactions with substrates. The similar directions of the frequency and dissipation profiles for 0.25% PLL indicate that during the process of removal of adsorbed Brij-35 by PLL from the Dursan surface, the *in-situ* molecular complex of Brij-35 – PLL that formed was viscoelastic in nature. For 1% PLL, the dissipation increased considerably during contact with the sensor and decreased to values of $\sim 0.5 \times 10^{-6}$ units upon rinse indicating slight viscoelastic nature of the PLL film formed on the Dursan surface. In case of PLL adsorption on bare SS sensor, the dissipation showed concentration dependent trends, atypical of macromolecular adsorption, during contact of all bulk solutions with the sensor. However, it reverted back to the baseline values upon rinse by WB1 indicating rigid nature of the adsorbed PLL film on SS surface. The $|\Delta D/\Delta f|$ values of $<0.1 \times 10^{-6}$ Hz^{-1} also provides confirmation of the rigid nature of the adsorbed PLL film (Table 4).

Adsorption of PLL on hydrophobic surfaces via interactions of the polypeptide alkyl backbone with the surface, and on hydrophilic surfaces via strong electrostatic interactions driven by opposite charges on the adsorbate and the substrate at neutral pH have been reported earlier [61–63]. As shown in Table 4, the amount of PLL adsorbed as a monolayer on SS in this study (i.e. $\sim$100 ng cm^{-2}) is roughly 3-fold and 5-fold lower than the values obtained by York et al. [61] and Barrantes et al. [62], respectively for adsorption on hydrophilic silica surface. It appears that the adsorbed amount varied directly with the average molecular weight of PLL used in the respective studies. The adsorbed amounts in all these studies were considerably greater than the values of $\sim$40 ng cm^{-2} reported by Jiang et al. [63] for even higher molecular weight PLL. The differences can be attributed to the measurement techniques, i.e. optical reflectometry [63] vs. QCM-D [61,62], that, as mentioned earlier, measures the coupled water content of the adsorbed protein film. York et al. [61] reported comparable adsorption of PLL on both the hydrophobic polystyrene and hydrophilic silica surfaces indicating that the surface hydrophilicity did not play a distinctive role in PLL adsorption.

In our study, the presence of a nonionic surfactant, Brij-35, was successful in weakening the hydrophobic interactions and preventing adsorption on Dursan surface at 0.25% or lower PLL concentrations at neutral pH. At higher PLL concentrations ($\geq$1%), considerable adsorption on Dursan can be attributed to the increased interfacial ordering of polymer backbones of densely

Table 4
QCM-D data for the poly-L-lysine-surface system with WB1 as baseline and rinse buffer. Mean (±SD) values of the 3rd overtone data with normalized frequency changes have been reported.

	Δf_3 (Hz)		ΔD_3 (1×10^{-6})		$\lvert\Delta D_3/\Delta f_3\rvert$ (10^{-6}Hz^{-1})		Sauerbrey Mass (ng/cm^2)		Sauerbrey thickness (nm)
Coating	Dursan	SS	Dursan	SS	Dursan	SS	Dursan	SS	SS
Protein									
0.1% PLL	0.56$^{(4)}$ (±0.5)	−5.63$^{(4)}$ (±0.7)	−0.01 (±0.1)	−0.15 (±0.1)	0.01	0.03	−9.89 (±9.5)	101** (±1.2)	0.9 (±0.1)
0.25% PLL	−0.94$^{(2)}$ (0.3)	−6.22$^{(2)}$ (±0.5)	0.17 (±0.0)	0.22 (±0.1)	0.18*	0.04	16.48 (±5.5)	109 (±9)	1.0 (±0.1)
1% PLL	−4.41$^{(4)}$ (0.7)	−6.06$^{(4)}$ (±0.5)	0.57 (±0.1)	−0.01 (±0.2)	0.13	0.00	79.13 (±12.5)	106 (±9)	1.0 (±0.1)

$^{(x)}$ number in parantheses represents number of measurements for a given protein-coating system.

* Although, $\lvert\Delta D_3/\Delta f_3\rvert$ values for Dursan coating were >0.1 × 10^{-6} Hz^{-1}, due to negligible frequency at rinse step, Sauerbrey equation was used to calculate the hypothetical surface mass of the adsorbed protein.

** Viscoelastic modeling of the data for adsorption of PLL at different concentrations on Stainless steel sensor was not carried out since, as shown in Supplementary Fig. S-F3, the frequency profiles at the rinse step did not show any separation, indicating rigid nature of the adsorbed PLL film.

charged PLL molecules at the hydrophobic interface. This increased ordering did not allow Brij-35 to weaken the hydrophobic interfacial interactions between PLL molecules and the Dursan surface, and thus led to retention of adsorbed PLL layer.

4. Conclusions

The protein resistant properties of a chemical vapor deposited hydrophobic alkyl-functional carboxy silane coating (Dursan®) on stainless steel were characterized using QCM-D. It was demonstrated that a nonionic surfactant, Brij-35 in the wash buffer was instrumental in facilitating easy removal of adsorbed immunoassay blocker proteins (BSA and mouse IgG) and normal human plasma proteins from the hydrophobic Dursan surface. On the other hand, Brij-35 did not alter adsorption behavior of these proteins on bare stainless steel surface. While it is not surprising that a stronger ionic- and hydrogen bonding would lead to more difficult removal of residual protein from the stainless steel surface by non-ionic detergent, these results however emphasize the need for design consideration of surfaces used in biotechnology applications, especially in analytical settings. The choice of hardware and interactive parts of any automated system should consider the available and compatible cleaning solutions used and the nature of the reagents handled. The practical data shown in this report shows that fast and significant adsorption within seconds is possible on either electrostatic or hydrophobic surfaces, thus implying the real nature of the problem faced, for example, by clinical labs using automated systems.

If automated analytical systems are to mitigate fouling to their parts in contact with samples and reagents, these should be challenged to understand their limitations. This was the reason for studying PLL, a synthetic cationic polymer that did not adsorb on the Dursan surface below certain solution concentrations, but resulted in surface fouling at a challenging high concentration. These observations should lead us to implement optional but suitable combinations of wash solutions for realistic scenarios to complement the improved surface. It is clear that the effect of solution pH on adsorption behavior of highly charged macromolecules remains to be further characterized.

It is now well understood that the combination of surface chemistry and the solution environment that a coating material is exposed to can lead to biofouling, which can be prevented using following three precautionary measures: (i) pre-exposure prevention, i.e. by modifying the surface chemistry to prevent non-specific adsorption; (ii) during-exposure prevention, i.e. by changing the solution properties such as pH, ionic strength, and by using excipients such as ionic and/or non-ionic surfactants to alter the electrostatic as well as hydrophobic interactions; and (iii) post-exposure prevention, i.e. by using wash/rinse solutions containing caustic chemicals and/or small molecular surface active agents. Any one of these measures on its own cannot provide a universal fix to the biofouling problem, but various combinations of these three can work. The combination of the durable and inert alkyl-functional carboxysilane coating (Dursan) and the non-ionic surfactant in the wash buffer that we have reported here is certainly a step forward in that direction, specifically in case of automated assay analyzers, reagent manufacturing, and filling setups.

Authors' contributions

The manuscript was written through contributions of all authors. All authors have given approval to the final version of the manuscript.

Acknowledgments

Ryan Bonn of Abbott Laboratories for capillary isoelectric focussing (CIEF) measurements and Tracy Wasilewski for the optical micrographs of the Dursan and AF1600 coated sensors.

Appendix A. Supplementary data

Supplementary data associated with this article can be found, in the online version, at http://dx.doi.org/10.1016/j.apsusc.2015.12.086.

References

[1] I. Banerjee, R.C. Pangule, R.S. Kane, Antifouling coatings: recent developments in the design of surfaces that prevent fouling by proteins, bacteria, and marine organisms, Adv. Mater. 23 (2011) 690–718.
[2] S. Krishnan, C.J. Weinman, C.K. Ober, Advances in polymers for anti-biofouling surfaces, J. Mater. Chem. 18 (2008) 3405–3413.
[3] A. Hucknall, S. Rangarajan, A. Chilkoti, In pursuit of zero: polymer brushes that resist the adsorption of proteins, Adv. Mater. 21 (2009) 2441–2446.
[4] E. Ostuni, R.G. Chapman, R.E. Holmlin, S. Takayama, G.M. Whitesides, A survey of structure–property relationships of surfaces that resist the adsorption of protein, Langmuir 17 (2001) 5605–5620.
[5] A. Roosjen, J. de Vries, H.C. van der Mei, W. Norde, H.J. Busscher, Stability and effectiveness against bacterial adhesion of poly(ethylene oxide) coatings in biological fluids, J. Biomed. Mater. Res. B 73 (2005) 347–354.
[6] S. Petronis, K. Berntsson, J. Gold, P. Gatenholm, Design and microstructuring of PDMS surfaces for improved marine biofouling resistance, J. Biomater. Sci. Polym. Ed. 11 (2000) 1051–1072.
[7] F. Höök, M. Rodahl, P. Brzezinski, B. Kasemo, Energy dissipation kinetics for protein and antibody–antigen adsorption under shear oscillation on a quartz crystal microbalance, Langmuir 14 (1998) 729–734.
[8] M.C. Dixon, Quartz crystal microbalance with dissipation monitoring: enabling real-time characterization of biological materials and their interactions, J. Biomol. Tech. 19 (2008) 151–158.
[9] D.A. Smith, J.B. Mattzela, P.H. Silvis, G.A. Barone, Chemical Vapor Deposition Coating, Article, and Method, *USPTO*, Application US 13/504,533 (2012).
[10] D.A. Smith, J.B. Mattzela, P.H. Silvis, G.A. Barone, M.E. Higgins, Wear Resistant Coating, Article, and Method, *USPTO*, Application US 13/876,328 (2013).
[11] T. Suzawa, Y. Ikariyama, M. Aizawa, New approach for sensitization of solid-phase immunoassay based on controlling of nonspecific binding:

combination of enzyme amplification and sensitive electrochemical detection, Anal. Sci. 9 (1993) 641–646.
[12] J. Tate, G. Ward, Interferences in immunoassay, Clin. Biochem. Rev. 25 (2004) 105–120.
[13] S.E. Cowan, D. Liepmann, J.D. Keasling, Development of engineered biofilms on poly-L-lysine patterned surfaces, Biotechnol. Lett. 23 (2001) 1235–1241.
[14] N.L. Anderson, N.G. Anderson, The human plasma proteome: history, character, and diagnostic prospects, Mol. Cell. Proteomics 1 (2002) 845–867.
[15] Y.S. Hedberg, M.S. Killian, E. Blomberg, S. Virtanen, P. Schmuki, I. Odnevall Wallinder, Interaction of bovine serum albumin and lysozyme with stainless steel studied by time-of-flight secondary ion mass spectrometry and X-ray photoelectron spectroscopy, Langmuir 28 (2012) 16306–16317.
[16] Y. Hedberg, X. Wang, J. Hedberg, M. Lundin, E. Blomberg, I.O. Wallinder, Surface-protein interactions on different stainless steel grades: effects of protein adsorption, surface changes and metal release, J. Mater. Sci.: Mater. Med. 24 (2013) 1015–1033.
[17] G. Sauerbrey, Verwendung von Schwingquarzen zur Wägung dünner Schichten und zur Mikrowägung, Z. Phys. 155 (1959) 206–222.
[18] M.V. Voinova, M. Rodahl, M. Jonson, B. Kasemo, Viscoelastic acoustic response of layered polymer films at fluid-solid interfaces: continuum mechanics approach, Phys. Scr. 59 (1999) 391.
[19] D. Wild, W. Kusnezow, Separation systems, in: D. Wild (Ed.), The Immunoassay Handbook, Elsevier Ltd, Oxford, UK, 2005, pp. 177–191.
[20] R.S. Sista, A.E. Eckhardt, V. Srinivasan, M.G. Pollack, S. Palanki, V.K. Pamula, Heterogeneous immunoassays using magnetic beads on a digital microfluidic platform, Lab Chip 8 (2008) 2188–2196.
[21] B. Jöhnson, M. Lund, F.L.B. da Silva, Electrostatics in macromolecular solution, in: E. Dickinson, M.E. Leser (Eds.), Food Colloids: Self-Assembly and Material Science, Royal Society of Chemistry, Cambridge, UK, 2007, pp. 129–154.
[22] S. Poole, S.I. West, J.C. Fry, Effects of basic proteins on the denaturation and heat-gelation of acidic proteins, Food Hydrocolloids 1 (1987) 301–316.
[23] H. Juvonen, A. Maattanen, P. Ihalainen, T. Viitala, J. Sarfraz, J. Peltonen, Enhanced protein adsorption and patterning on nanostructured latex-coated paper, Colloids Surf. B 118 (2014) 261–269.
[24] R.J. Marsh, R.A.L. Jones, M. Sferrazza, Adsorption and displacement of a globular protein on hydrophilic and hydrophobic surfaces, Colloids Surf. B 23 (2002) 31–42.
[25] J. Jin, W. Jiang, J. Yin, X. Ji, P. Stagnaro, Plasma proteins adsorption mechanism on polyethylene-grafted poly(ethylene glycol) surface by quartz crystal microbalance with dissipation, Langmuir 29 (2013) 6624–6633.
[26] C.F. Wertz, M.M. Santore, Adsorption and relaxation kinetics of albumin and fibrinogen on hydrophobic surfaces: single-species and competitive behavior, Langmuir 15 (1999) 8884–8894.
[27] S.V. Vaidya, A.R. Narváez, Understanding interactions between immunoassay excipient proteins and surfactants at air–aqueous interface, Colloids Surf. B 113 (2014) 285–294.
[28] A.P. Gunning, A.R. Mackie, P.J. Wilde, V.J. Morris, In situ observation of the surfactant-induced displacement of protein from a graphite surface by atomic force microscopy, Langmuir 15 (1999) 4636–4640.
[29] F. Höök, B. Kasemo, T. Nylander, C. Fant, K. Sott, H. Elwing, Variations in coupled water, viscoelastic properties, and film thickness of a Mefp-1 protein film during adsorption and cross-linking: a quartz crystal microbalance with dissipation monitoring, ellipsometry, and surface plasmon resonance study, Anal. Chem. 73 (2001) 5796–5804.
[30] M.P. Gispert, A.P. Serro, R. Colaço, B. Saramago, Bovine serum albumin adsorption onto 316L stainless steel and alumina: a comparative study using depletion, protein radiolabeling, quartz crystal microbalance and atomic force microscopy, Surf. Interface Anal. 40 (2008) 1529–1537.
[31] L.M. Pandey, S.K. Pattanayek, D. Delabouglise, Properties of adsorbed bovine serum albumin and fibrinogen on self-assembled monolayers, J. Phys. Chem. C 117 (2013) 6151–6160.
[32] D.C. Carter, J.X. Ho, Structure of serum albumin, Adv. Protein Chem. 45 (1994) 153–203.
[33] S. Sugio, A. Kashima, S. Mochizuki, M. Noda, K. Kobayashi, Crystal structure of human serum albumin at 2.5 Å resolution, Protein Eng. 12 (1999) 439–446.
[34] M.L. Ferrer, R. Duchowicz, B. Carrasco, J.G. de la Torre, A.U. Acuña, The conformation of serum albumin in solution: a combined phosphorescence depolarization-hydrodynamic modeling study, Biophys. J. 80 (2001) 2422–2430.
[35] I. Kiesel, M. Paulus, J. Nase, S. Tiemeyer, C. Sternemann, K. Rüster, F.J. Wirkert, K. Mende, T. Büning, M. Tolan, Temperature-driven adsorption and desorption of proteins at solid–liquid interfaces, Langmuir 30 (2014) 2077–2083.
[36] G.V. Lubarsky, M.R. Davidson, R.H. Bradley, Hydration-dehydration of adsorbed protein films studied by AFM and QCM-D, Biosens. Bioelectron. 22 (2007) 1275–1281.
[37] F. Zhang, M.W.A. Skoda, R.M.J. Jacobs, S. Zorn, R.A. Martin, C.M. Martin, G.F. Clark, S. Weggler, A. Hildebrandt, O. Kohlbacher, F. Schreiber, Reentrant condensation of proteins in solution induced by multivalent counterions, Phys. Rev. Lett. 101 (2008) 148101.
[38] J. Voros, The density and refractive index of adsorbing protein layers, Biophys. J. 87 (2004) 553–561.
[39] M. Dąbkowska, Z. Adamczyk, Mechanism of immonoglobulin G adsorption on mica-AFM and electrokinetic studies, Colloids Surf. B 118 (2014) 57–64.
[40] K. Awsiuk, A. Bernasik, M. Kitsara, A. Budkowski, P. Petrou, S. Kakabakos, S. Prauzner-Bechcicki, J. Rysz, I. Raptis, Spectroscopic and microscopic characterization of biosensor surfaces with protein/amino-organosilane/silicon structure, Colloids Surf. B 90 (2012) 159–168.
[41] J. Buijs, J.W.T. Lichtenbelt, W. Norde, J. Lyklema, Adsorption of monoclonal IgGs and their F(ab′)2 fragments onto polymeric surfaces, Colloids Surf. B 5 (1995) 11–23.
[42] C. Dupont-Gillain, Orientation of adsorbed antibodies: in situ monitoring by QCM and random sequential adsorption modeling, in: T. Horbett, J.L. Brash, W. Norde (Eds.), Proteins at Interfaces III State of the Art, American Chemical Society, Washington, DC, USA, 2012, pp. 453–469.
[43] J.S. Bee, M. Davis, E. Freund, J.F. Carpenter, T.W. Randolph, Aggregation of a monoclonal antibody induced by adsorption to stainless steel, Biotechnol. Bioeng. 105 (2010) 121–129.
[44] C. Zhou, J.-M. Friedt, A. Angelova, K.-H. Choi, W. Laureyn, F. Frederix, L.A. Francis, A. Campitelli, Y. Engelborghs, G. Borghs, Human immunoglobulin adsorption investigated by means of quartz crystal microbalance dissipation, atomic force microscopy, surface acoustic wave, and surface plasmon resonance techniques, Langmuir 20 (2004) 5870–5878.
[45] M. Rodahl, F. Hook, C. Fredriksson, C.A. Keller, A. Krozer, P. Brzezinski, M.V. Voinova, B. Kasemo, Simultaneous frequency and dissipation factor QCM measurements of biomolecular adsorption and cell adhesion, Faraday Discuss. 107 (1997) 229–246.
[46] Y.S. Sun, J.P. Landry, Y.Y. Fei, X.D. Zhu, J.T. Luo, X.B. Wang, K.S. Lam, Macromolecular scaffolds for immobilizing small molecule microarrays in label-free detection of protein–ligand interactions on solid support, Anal. Chem. 81 (2009) 5373–5380.
[47] K. Wadu-Mesthrige, N.A. Amro, G.-Y. Liu, Immobilization of proteins on self-assembled monolayers, Scanning 22 (2000) 380–388.
[48] C.J. Frégeau, C. Marc Lett, J. Elliott, C. Yensen, R.M. Fourney, Automated processing of forensic casework samples using robotic workstations equipped with nondisposable tips: contamination prevention, J. Forensic Sci. 53 (2008) 632–651.
[49] M. Iten, R. Weibel, I. König, R. Beckbissinger, T. Benthien, W. Hälg, N. Ingenhoven, A. Lehnert, L. Oeltjen, C. Zaborosch, Reduction of carry over in liquid-handling systems with a decontamination step integrated in the washing procedure, JALA 15 (2010) 379–389.
[50] A.L. Lim, R. Bai, Membrane fouling and cleaning in microfiltration of activated sludge wastewater, J. Membr. Sci. 216 (2003) 279–290.
[51] M. Kazemimoghadam, T. Mohammadi, Chemical cleaning of ultrafiltration membranes in the milk industry, Desalination 204 (2007) 213–218.
[52] G. Speranza, G. Gottardi, C. Pederzolli, L. Lunelli, R. Canteri, L. Pasquardini, E. Carli, A. Lui, D. Maniglio, M. Brugnara, M. Anderle, Role of chemical interactions in bacterial adhesion to polymer surfaces, Biomaterials 25 (2004) 2029–2037.
[53] P.A.E. Piunno, U.J. Krull, R.H.E. Hudson, M.J. Damha, H. Cohen, Fiber-optic DNA sensor for fluorometric nucleic acid determination, Anal. Chem. 67 (1995) 2635–2643.
[54] F. Benítez, E. Martínez, M. Galán, J. Serrat, J. Esteve, Mechanical properties of plasma deposited polymer coatings, Surf. Coat. Technol. 125 (2000) 383–387.
[55] H. Chen, O. Jacobs, W. Wu, G. Rüdiger, B. Schädel, Effect of dispersion method on tribological properties of carbon nanotube reinforced epoxy resin composites, Polym. Test. 26 (2007) 351–360.
[56] J.A. Lee, T.J. McCarthy, Preparation of ultrahydrophilic surfaces via oxidation reactions of silicon wafer-supported alkylsilane monolayers, Polym. Preprints 46 (2005) 791–792.
[57] T.M. Owens, B.J. Ludwig, K.S. Schneider, D.R. Fosnacht, B.G. Orr, M.M. Holl, Oxidation of alkylsilane-based monolayers on gold, Langmuir 20 (2004) 9636–9645.
[58] J.A. Lee, T.J. McCarthy, Polymer surface modification: topography effects leading to extreme wettability behavior, Macromolecules 40 (2007) 3965–3969.
[59] K. Senda, T. Matsuda, K. Tanaka, Improvement of adhesion strength of fluoropolymer thin films by vapor deposition polymerization, IEICE Trans. Electron. E96-C (2013) 374.
[60] R.L. Scopp, D.M. Finley, K.L. Trimpe, A. Lach, C.D. Pestel, J.M. Ramp, Methods and Kits for Decreasing Interferences of Assay Samples Containing Plasma or Serum in Specific Binding Assays by using a Large Polycation *USPTO*, US 2013/0011827 A1 (2013) 1–6.
[61] R.L. York, G.J. Holinga, G.A. Somorjai, An investigation of the influence of chain length on the interfacial ordering of L-lysine and L-proline and their homopeptides at hydrophobic and hydrophilic interfaces studied by sum frequency generation and quartz crystal microbalance, Langmuir 25 (2009) 9369–9374.
[62] A. Barrantes, O. Santos, J. Sotres, T. Arnebrant, Influence of pH on the build-up of poly-L-lysine/heparin multilayers, J. Colloid Interface Sci. 388 (2012) 191–200.
[63] M. Jiang, I. Popa, P. Maroni, M. Borkovec, Adsorption of poly(L-lysine) on silica probed by optical reflectometry, Colloids Surf. A 360 (2010) 20–25.